



ELSEVIER

Journal of Chromatography A, 728 (1996) 113–128

JOURNAL OF
CHROMATOGRAPHY A

Immobilized-artificial-membrane chromatography: measurements of membrane partition coefficient and predicting drug membrane permeability

Shaowei Ong, Hanlan Liu, Charles Pidgeon*

Department of Medicinal Chemistry, School of Pharmacy, Purdue University, West Lafayette, IN 47907, USA

Abstract

Immobilized artificial membranes (IAMs) are chromatographic surfaces prepared by covalently immobilizing cell membrane phospholipids to solid surfaces at monolayer densities. IAM surfaces mimic fluid cell membranes. For 23 structurally unrelated compounds, solute capacity factors [$\log(k'_{IAM})$] measured on IAM columns correlate very well with the solute equilibrium partition coefficients [$\log(K_m)$] measured in fluid liposome systems ($r = 0.907$). This indicates that solute partitioning between the IAM bonded phase and the aqueous mobile phase is similar to the solute partitioning between liposomes and the aqueous phase. IAMs also predicted oral drug absorption in mice and drug permeability through Caco-2 cells. IAM chromatography is experimentally simple and large volume screening of experimental compounds for drug absorption is possible. Solute retention on IAMs was found to be dominated by a partitioning mechanism. The structural requirements for HPLC bonded phases to predict solute–membrane partitioning are briefly discussed.

Keywords: Immobilized artificial membranes; Partition coefficients; Drug transport; Membrane permeability; Membranes; Retention mechanisms.

1. Introduction

The interactions of biomolecules with cell membranes are common biological processes. Solute–membrane interactions are characterized by membrane partition coefficients (K_m) which represent the solute distribution between the aqueous phase and the membrane. The free energy (ΔG_m^0) of solute–membrane interactions is related to K_m as follows:

$$\Delta G_m^0 = -RT \ln(K_m) \quad (1)$$

* Corresponding author.

Therefore, the membrane partition coefficient (K_m) represents all possible molecular interactions between a solute and the membrane, and is thus of great importance to many biological processes. For instance, evaluating membrane partition coefficients is a critical step in the drug discovery process. Drug activity, drug toxicity, drug distribution, and other processes depend on drug absorption, which often depends on drug membrane partitioning. This is because the major absorption barrier to drugs given orally is the gastrointestinal cell membranes and most drugs given orally are absorbed across the intestinal mucosa by a passive diffusion mechanism [1].

For drugs absorbed by a passive diffusion mechanism, the permeability, P_m , of a drug through the membrane is directly proportional to K_m [2]:

$$P_m = \frac{D_m K_m}{L} \quad (2)$$

where D_m is the membrane diffusion coefficient of the solute and L is the membrane thickness.

Because of the importance of K_m in the drug discovery process and many other biological processes, measurements of K_m have been the subject of many studies for the last several decades. However, K_m is difficult to measure in vivo and therefore three in vitro membrane systems have been developed to model solute–membrane partitioning. The three models include simple organic-solvent–aqueous partitioning systems, such as octanol–water partitioning systems [3–5], chromatographic partitioning systems using octadecyl silica (ODS) as a stationary phase [6–8], and liposome partitioning systems [9–11].

It should be noted that partitioning of a drug into a cell membrane results from all possible molecular drug–membrane interactions. However, octanol–water partitioning systems and ODS chromatography can model only the hydrophobic contribution of drug–membrane interactions, whereas the interactions between solutes and the polar lipid head groups are not modeled [12]. In contrast to simple organic solvents or ODS chromatography surfaces, liposome suspensions prepared from phospholipids exhibit structural similarities to the phospholipid bilayer found in cell membranes. It has been shown that solute partitioning into liposomes is virtually identical to solute partitioning into cell plasma membranes [13]. In addition, liposome partition coefficients have been used to study many solute–membrane interactions [14], and numerous QSAR studies have successfully correlated drug activities with drug liposome partition coefficients [15–17].

Although liposomes can model solute partitioning into cell membranes [13], there are many experimental duties that limit the wide-scale development of liposomes as an in vitro model for predicting drug–membrane interactions.

Limitations of the liposome system stem from the procedure of (i) liposome preparation, followed by (ii) solute equilibration in the liposome suspension, followed by (iii) quantitation of the free solute in the presence of liposomes, and (iv) the correction for the amount of drug that has partitioned into the aqueous space of the liposomes. The liposome method is thus time-consuming and tedious, and if many compounds are under evaluation, then it is not feasible to measure the equilibrium liposome partitioning coefficient for all of the compounds. In addition, significant amounts of compounds are needed for study unless radiolabeled analogs are available. It is thus prohibited to perform large-scale screening with regard to solute–membrane partitioning using the liposome model.

Immobilized artificial membranes (IAMs) are solid-phase-membrane-mimetics whereby cell membrane phospholipid molecules are covalently bonded to silica particles at high molecular surface densities. Compared to liposome or octanol–water partitioning systems, IAM chromatography in which IAMs are used as a HPLC stationary phase is experimentally much simpler. Using IAM chromatography to measure the solute partition coefficient between the aqueous phase and the IAM bonded phase (K_{IAM}) only requires the measurements of retention time of the solute (t_R) on the IAM HPLC column. The retention times (t_R) of solute molecules on IAM columns are used to calculate the solute IAM capacity factors k'_{IAM} using the following equation:

$$k'_{IAM} = \frac{t_R - t_0}{t_0} \quad (3)$$

where t_R is the retention time in minutes of the test compound and t_0 corresponds to the column dead time or void volume. The IAM capacity factor, k' , is linearly related to the equilibrium IAM partition coefficient, K_{IAM} :

$$k'_{IAM} = \frac{V_s}{V_m} K_{IAM} = \phi K_{IAM} \quad (4)$$

where V_m is the total volume of solvent within the IAM HPLC column, V_s is the volume of the IAM interphase created by the immobilized phospholipids, and $\phi = V_s/V_m$ is the phase ratio,

which is a constant for a given IAM column. It is clear from Eq. 4 that by measuring k'_{IAM} one can determine the solute partition coefficient into the IAM interphase; the IAM interphase is physically an immobilized liquid formed by the conglomerate of the bonded lipids.

The molecular basis for using IAM chromatography to predict solute partitioning into fluid membranes is that IAMs are physically similar to, and therefore mimic, fluid phospholipid bilayers. IAMs have monolayer surface densities of immobilized phospholipids similar to liposome membranes [18,19]. IAMs also exhibit similar interfacial motional properties compared to the motional properties of the mobile lipids in fluid liposomes, as revealed by our recent ^{31}P NMR studies [20,21]. These physical similarities between IAMs and fluid membranes encouraged us to evaluate if IAM partition coefficients, K_{IAM} , are correlated with the equilibrium membrane partition coefficient K_m of solute partitioning into liposome membranes.

This paper reviews our recent work on (i) validating if K_{IAM} correlates K_m [22], (ii) application of IAM chromatography in predicting drug transport through membranes using IAM chromatography [23], (iii) the mechanism of the solute retention on IAM columns [24], and (iv) studies of the structural requirements for HPLC bonded phases to model solute–membrane interactions [12].

2. Experimental section

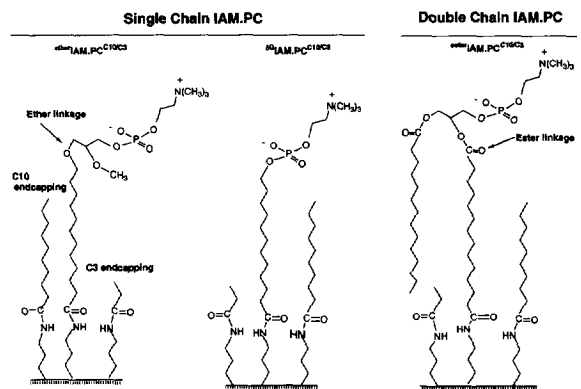
2.1. Chemicals

The following chemicals were purchased from Sigma: phenol, *p*-cresol, *p*-ethylphenol (Et-phenol), *p*-*n*-propylphenol (Pr-phenol), *p*-fluorophenol (F-phenol), *p*-chlorophenol (Cl-phenol), *p*-bromophenol (Br-phenol), *p*-iodophenol (I-phenol), xylometazoline, oxy-metazoline, naphazoline, tetrahydrozoline, clonidine, propranolol hydrochloride, alprenolol, oxprenolol, metoprolol, pindolol, nadolol, atenolol, tolazoline, and phosphate-buffered saline (PBS). *p*-*n*-Butylphenol (Bu-phenol) was

purchased from Lancaster. The following drugs were kindly provided by Boehringer-Ingelheim STH2224, STH2100, ST606, ST476, ST585, ST590, ST608, ST475, ST603, ST600, and tramazoline. Phenethylamine derivatives, including MESC, ESC, PROSC, ISOPROSC, BROSC, 2C-T, DOT, DON, DOB, DOM, DOET, DOPR, DOBU, and DOAM, were kindly provided by Dr. D. Nichols of Department of Medicinal Chemistry at Purdue University. Cephalosporin prodrugs were kindly provided by Eli Lilly and Co.

2.2. Synthesis of IAM.PC bonded phases

As shown in Scheme 1, three IAM bonded phases were prepared from three different phosphatidylcholine ligands: (i) a single chain ether PC ligand ($^{\text{ether}}\text{IAM.PC}^{C_{10}/C_3}$); (ii) a single chain PC ligand that lacks a glycerol backbone ($^{\delta G}\text{IAM.PC}^{C_{10}/C_3}$); and (iii) a diacylated or double chain PC ligand ($^{\text{ester}}\text{IAM.PC}^{C_{10}/C_3}$). Single chain IAM.PC denotes either $^{\text{ether}}\text{IAM.PC}^{C_{10}/C_3}$ or $^{\delta G}\text{IAM.PC}^{C_{10}/C_3}$, double chain IAM.PC denotes $^{\text{ester}}\text{IAM.PC}^{C_{10}/C_3}$. $^{\delta G}\text{IAM.PC}^{C_{10}/C_3}$ is currently commercialized as an IAM.PC.DD column (Regis Technologies). Detailed procedures for the synthesis of IAM.PC bonded phases have been described for the $^{\text{ether}}\text{IAM.PC}^{C_{10}/C_3}$ phase [19], the IAM.PC.DD phase [22], and the $^{\text{ester}}\text{IAM.PC}^{C_{10}/C_3}$ phase [25]. Table 1 shows the bonded ligand densities of these three IAM.PC phases, which were measured as described [18].



Scheme 1.

Table 1
Ligand density on $^{\text{ether}}\text{IAM.PC}^{\text{C}_{10}/\text{C}_3}$, $^{\delta\text{G}}\text{IAM.PC}^{\text{C}_{10}/\text{C}_3}$, and $^{\text{ester}}\text{IAM.PC}^{\text{C}_{10}/\text{C}_3}$ surfaces

IAM.PC phase	PC ligand		C ₁₀		C ₃	
	$\mu\text{mol-PC/g-IAM}$	mg-PC/g-IAM	$\mu\text{mol-C}_{10}/\text{g-IAM}$	$\text{mg-C}_{10}/\text{g-IAM}$	$\mu\text{mol-C}_3/\text{g-IAM}$	$\text{mg-C}_3/\text{g-IAM}$
$^{\text{ether}}\text{IAM.PC}^{\text{C}_{10}/\text{C}_3}$	127.0	59.7	28.0	3.9	60.0	2.5
$^{\delta\text{G}}\text{IAM.PC}^{\text{C}_{10}/\text{C}_3}$	127.0	48.5	48.0	6.7	36	1.5
$^{\text{ester}}\text{IAM.PC}^{\text{C}_{10}/\text{C}_3}$	98	70.0	48.6	6.7	28	1.2

2.3. IAM chromatography

All HPLC columns containing IAM stationary phases were packed at Regis Technologies. IAM HPLC columns were either 15×0.46 cm with a void volume V_m of ca. 1.850 ml or 3×0.46 cm with a void volume V_m of ca. 0.415 ml. For all studies, the injection volume was ca. 10 μl of a solute aqueous solution (ca. 1 $\mu\text{g}/\mu\text{l}$), whereas for solutes that have low solubility in water the injection volume was ca. 10 μl of a solute-methanol solution. The buffered aqueous mobile phase was 0.01 M PBS at pH 7.4 (which contains 0.027 M of KCl, and 0.137 M of NaCl). The flow-rate was 1, 2, or 3 ml/min and solute detection was at 220 nm. Chromatograms were obtained using a Rainin HPLC pumping system equipped with a Knauer Model 87 detector and interfaced with a Macintosh computer. Rainin Dynamax software was used to record the chromatograms on the computer.

3. Results and discussion

3.1. Membrane partition coefficients chromatographically measured using IAM surfaces

To validate the idea that IAM chromatography can be used to measure solute-membrane partition coefficients, k'_{IAM} of 23 solutes were compared to the liposome partition coefficients K_m measured by Rogers et al. [15,17,26] using dimyristoylphosphatidylcholine (DMPC) liposomes (Fig. 1). The structures of these 23 solutes are given in Scheme 2. It is clear from Scheme 2

that these 23 solutes are structurally unrelated molecules, and therefore many different solute-membrane interactions are involved in the solute-membrane partitioning process. As shown in Fig. 1, $\log(k'_{\text{IAM}})$ vs. $\log(K_m)$ exhibits an excellent linear correlation with $r = 0.907$. It should be noted that the slope of the plot of $\log(k'_{\text{IAM}})$ vs. $\log(K_m)$ is very close to 1 (slope = 0.994), which indicates that k'_{IAM} is linearly proportional to K_m .

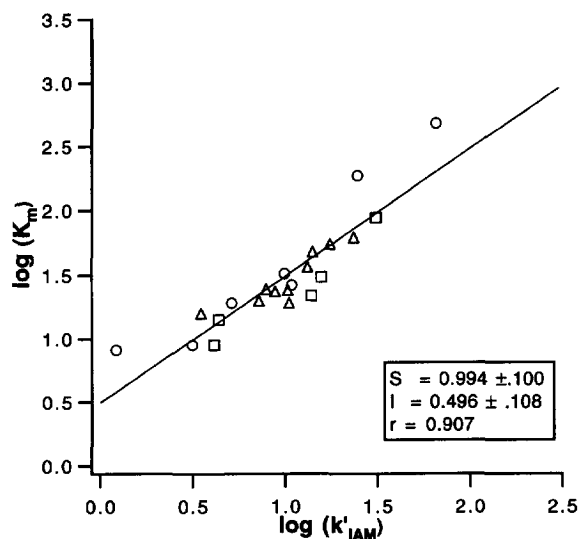
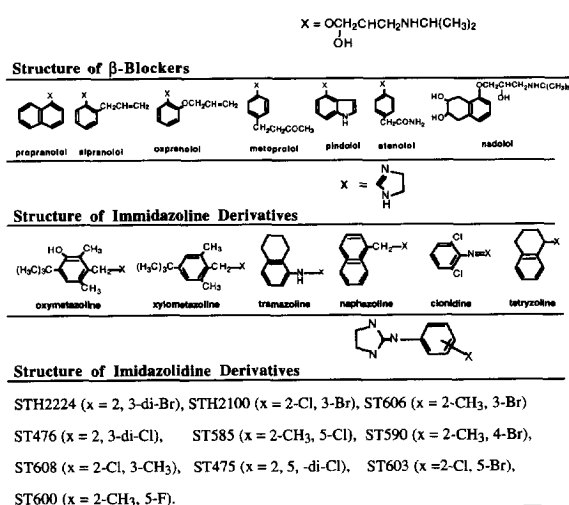


Fig. 1. Correlation of solute partitioning into DMPC liposomes [$\log(K_m)$] with solute binding $^{\text{ether}}\text{IAM.PC}^{\text{C}_{10}/\text{C}_3}$ surfaces [$\log(k'_{\text{IAM}})$] for seven β -blockers (O), six imidazoline derivatives (□), and ten imidazolidine derivatives (Δ) shown in Scheme 2. The liposome partition coefficients of these 23 solutes were measured using DMPC liposomes dispersed in 0.01 M PBS buffer (pH 7.4) [15,17,26]. IAM capacity factors, k'_{IAM} , were measured on a 15×0.46 cm $^{\text{ether}}\text{IAM.PC}^{\text{C}_{10}/\text{C}_3}$ column using a mobile phase of 0.01 M PBS (pH 7.4).



Scheme 2.

The IAM capacity factors k'_{IAM} can be used to calculate the K_{IAM} values which reflect the distribution of solute between the stationary phase and the mobile phase according to Eq. 4. However, the calculation of K_{IAM} from experimentally measured capacity factors, k'_{IAM} , requires a known value of the phase ratio (ϕ), or a known value of the volume of the stationary phase (V_s). The IAM interfacial thickness is unknown and it is therefore difficult to accurately calculate V_s ; approximations are thus made. Following the conventional method of calculating V_s on C₁₈ columns [27], the volume of the stationary phase (V_s) of an IAM.PC column is assumed to be the sum of the volume of bonded PC ligands (V_s^{PC}), the volume of bonded C₁₀ groups ($V_s^{\text{C}_{10}}$) and the volume of bonded C₃ groups ($V_s^{\text{C}_3}$). The volume of each individual bonded ligand was thus calculated as the weight of the ligand divided by the ligand's density:

$$V_s = V_s^{\text{PC}} + V_s^{\text{C}_{10}} + V_s^{\text{C}_3} = \frac{W^{\text{PC}}}{\rho^{\text{PC}}} + \frac{W^{\text{C}_{10}}}{\rho^{\text{C}_{10}}} + \frac{W^{\text{C}_3}}{\rho^{\text{C}_3}} \quad (5)$$

The density of the PC ligands (ρ^{PC}) is ca. 1.01 g/ml [11]. The density of hydrocarbons ($\rho^{\text{C}_{10}}$ and ρ^{C_3}) is ca. 0.86 g/ml [28]. Using the bonded ligand densities in Table 1, the phase ratio ($\phi =$

V_s/V_m) for the ether IAM.PC^{C₁₀/C₃} used in this work was determined to be 0.046 [24].

By using the phase ratio of 0.046 for the ether IAM.PC^{C₁₀/C₃} column, the K_{IAM} values were thus calculated according to Eq. 4. Based on the results of linear regression analysis shown in Fig. 1, the relationship between the liposome partition coefficient (K_m) and IAM partition coefficient (K_{IAM}) is:

$$K_{\text{IAM}} = (6.9 \pm 1.5)K_m \quad (6)$$

Eq. 6 indicates that solute partitioning into ether IAM.PC^{C₁₀/C₃} phase is about 7 times higher than solute partitioning into DMPC liposomes. Higher solute partitioning into the ether IAM.PC^{C₁₀/C₃} surface is most likely because ether IAM.PC^{C₁₀/C₃} has a lower PC density (ca. 85 Å/PC) [19,21] compared to the PC density in DMPC liposomes (ca. 62 Å/PC) [29] and thus exhibits a lower interfacial barrier when solutes partition into the lipid hydrocarbon region. This is further discussed below.

Solute partitioning into liposomes was next compared to solute partitioning using conventional octanol–water systems. Fig. 2A shows that the correlation between the log (K_m) and the log (K_{oct}) is very poor with a linear correlation coefficient $r = 0.520$. The correlation between log (k'_{IAM}) and log (K_{oct}) is also very poor with a linear correlation coefficient, $r = 0.454$ (Fig. 2B). Since the liposome partitioning system did not correlate with the octanol–aqueous partitioning system (Fig. 2A), the IAM partitioning system was also not expected to correlate either (Fig. 2B). This is because solute partitioning into liposomes and IAMs is virtually identical (Fig. 1). It should be emphasized that when non-polar interactions between solutes and membranes dominate the membrane binding energy, then both K'_m and k'_{IAM} are expected to correlate with K_{oct} . Using only the hydrophobic β -blockers as a subset of the 23 solutes, this can be clearly seen in Fig. 2C and D; log (K_m) correlates with log (K_{oct}) with $r = 0.957$ (Fig. 2C), and log (k'_{IAM}) correlates with log (K_{oct}) with $r = 0.883$ (Fig. 2D).

The key concept from Fig. 2 is that when hydrophobic interactions dominate the mem-

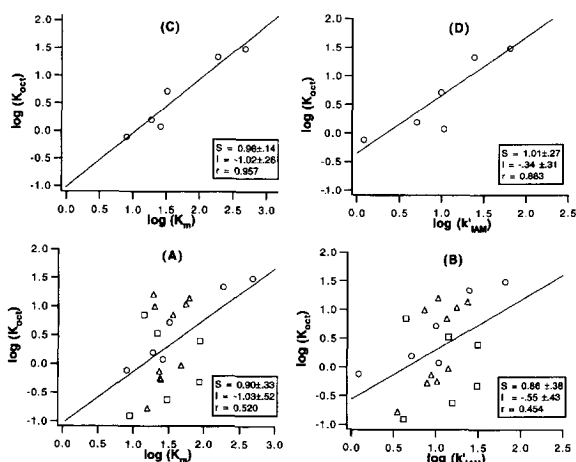


Fig. 2. Comparison of solute partitioning in an octanol–buffer system [$\log(K_{oci})$] and solute binding to $^{ether}IAM.PC^{C_{10}/C_3}$ surfaces [$\log(k'_{IAM})$] for seven β -blockers (\circ), six imidazoline derivatives (\square), and ten imidazolidine derivatives (\triangle) shown in Scheme 2. The octanol–buffer partition coefficients of these 23 solute molecules were measured by Rogers and co-workers with use of a 0.01 M PBS buffer (pH 7.4) [15,17,26]. The liposome partition coefficients of these 23 solutes were measured using DMPC liposomes in 0.01 M PBS buffer (pH 7.4) [15,17,26]. IAM capacity factors, k'_{IAM} , were measured on a 15×0.46 cm $^{ether}IAM.PC^{C_{10}/C_3}$ column using a mobile phase of 0.01 M PBS (pH 7.4).

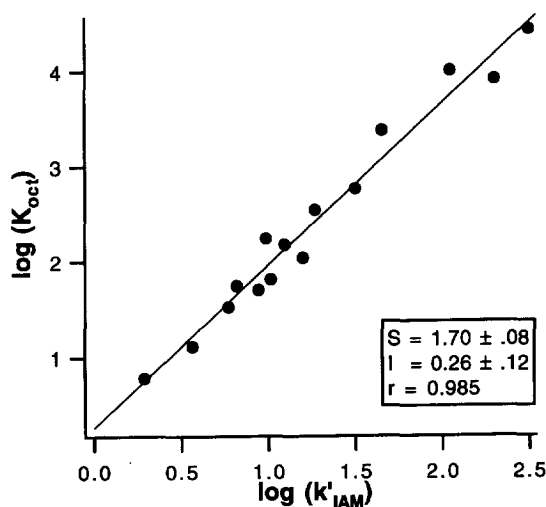


Fig. 3. Correlation of solute partitioning in an octanol–buffer system [$\log(K_{oci})$] with solute partitioning into $^{ether}IAM.PC^{C_{10}/C_3}$ [$\log(k'_{IAM})$] for 15 phenethylamine derivatives. The octanol–buffer partition coefficients were measured using an aqueous phase buffered at pH 8.0 [32]. IAM capacity factors, k'_{IAM} , were measured on a 15×0.46 cm $^{ether}IAM.PC^{C_{10}/C_3}$ column using a mobile phase of 0.01 M PBS at pH 7.4. The structures of the phenethylamine derivatives are shown in Table 2.

brane binding energy then octanol–water partition methods give the same results as IAM methods. This was verified on another set of compounds, phenylethylamine derivatives, as shown in Fig. 3; $\log(k'_{IAM})$ correlates with $\log(K_{oci})$ with a linear correlation coefficient, $r = 0.995$. As shown in Table 2, these fifteen phenethylamine derivatives are all very hydrophobic, and they are expected to interact predominantly with the non-polar hydrophobic chains of the lipid bilayer. Therefore, for a homologous series of hydrophobic solutes which interact mainly with the non-polar part of the lipid bilayer, K_{oci} usually correlates well with K_m or k'_{IAM} . However, for chemical structures that have polar functional groups that interact with polar lipid headgroups during solute partitioning, K_{oci} does not correlate well with K_m or k'_{IAM} (as shown in Figs. 2A and 2B).

In summary, solute partitioning into fluid liposome membranes can be modeled by solute partitioning into IAMs as shown in Scheme 3.

3.2. Predicting drug membrane permeability

After establishing that IAM chromatography can be used as a simple and rapid method to measure membrane partition coefficients, we evaluated if IAM chromatography is useful for predicting oral drug absorption. Measurements of oral drug absorption in animals requires extensive experimental effort, and thus is not suitable for screening large numbers of experimental compounds for absorption. As alternatives, a number of in vitro models, such as Caco-2 cell [1] and rat small intestine for predicting drug oral absorption [30] have been developed. We evaluated the usefulness of IAM chromatography in predicting drug oral absorption by correlating the drug partitioning into IAMs with drug intestinal permeability predicted by the Caco-2 cell model, drug intestinal absorption predicted by the rat small intestine model, and oral drug absorption in mice.

The human intestinal Caco-2 cell line has

Table 2
Structures of phenethylamine derivatives

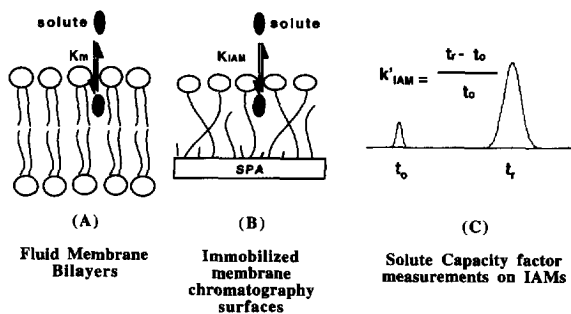


Phenethylamine derivatives	R ₂	R ₃	R ₄	R ₅	R
MESC	H	OCH ₃	OCH ₃	OCH ₃	H
ESC	H	OCH ₃	OC ₂ H ₅	OCH ₃	H
PROSC	H	OCH ₃	OC ₃ H ₇	OCH ₃	H
ISOPROSC	H	C ₃ H ₇	OiC ₃ H ₇	OCH ₃	H
BROSC	H	OCH ₃	Br	OCH ₃	H
2C-T	OCH ₃	H	SCH ₃	OCH ₃	H
DOT	OCH ₃	H	SCH ₃	OCH ₃	CH ₃
DON	OCH ₃	H	NO ₂	OCH ₃	CH ₃
DOB	OCH ₃	H	Br	OCH ₃	CH ₃
DOM	OCH ₃	H	CH ₃	OCH ₃	CH ₃
DOET	OCH ₃	H	C ₂ H ₅	OCH ₃	CH ₃
DOPR	OCH ₃	H	n-C ₃ H ₇	OCH ₃	CH ₃
DOBU	OCH ₃	H	n-C ₄ H ₉	OCH ₃	CH ₃
DOAM	OCH ₃	H	n-C ₅ H ₁₁	OCH ₃	CH ₃
DOTB	OCH ₃	H	t-C ₄ H ₉	OCH ₃	CH ₃

provided an in vitro cellular epithelium model to predict the intestinal permeability of drugs [1]. Artursson and Karlsson have shown that drug permeability in the Caco-2 cell model can be used to predict drug absorption in humans and thus the Caco-2 cell model can be used to screen for drug absorption prior to clinical trials [1]. Fig. 4 shows the correlation of the logarithm of the capacity factors (k'_{IAM}) of eleven drugs measured on an ^{ether}IAM.PC^{C₁₀/C₃} column with the

logarithm of the intestinal permeability coefficients (P_m) of the eleven drugs through Caco-2 cells as measured by Artursson and Karlsson [1]. For this group of eleven structurally diverse drugs, $\log(k'_{IAM})$ correlates with $\log(P_m)$ with a linear correlation coefficient $r = 0.762$. Based on Fig. 2, drug partitioning into IAMs, as measured chromatographically, correlates well with the intestinal permeability of drugs measured in the Caco-2 cell model.

To further evaluate the usefulness of IAM chromatography, a comparison was made of twelve drugs evaluated by Schanker et al. [30] using a perfused rat small intestinal model which measures the percent absorption (% Int Abs) at the actual tissue site. For this group of structurally diverse molecules, the correlation of $\log(\% \text{ Int Abs})$ vs. $\log(k'_{IAM})$ was $r = 0.791$ (Fig. 5A). For comparison, the accepted ODS chromatographic method for measuring lipophilicity was also used and a correlation of $r = 0.10$ was obtained using the same aqueous mobile phase (Fig. 5B).



Scheme 3.

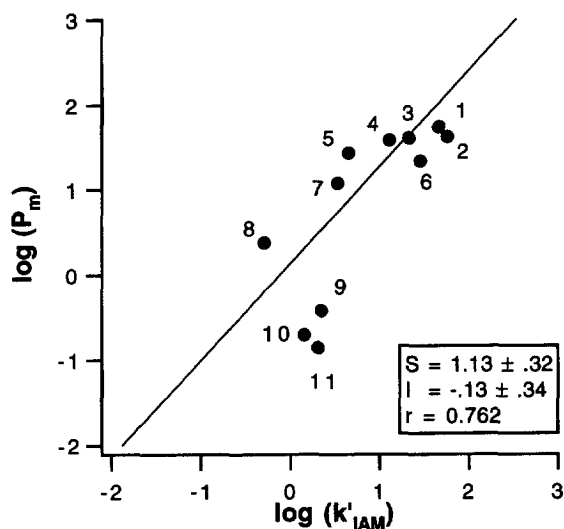


Fig. 4. Correlation of drug partitioning into an $\text{ether-IAM.PC}_{10/C_3}$ column [$\log(k'_{IAM})$] with drug intestinal permeability [$\log(P_m)$] through Caco-2 cells measured by Artursson and Karlsson [1] for the following eleven drugs: 1 = corticosterone; 2 = propranolol; 3 = alprenolol; 4 = warfarin; 5 = metoprolol; 6 = hydrocortisone; 7 = salicylic acid; 8 = acetylsalicylic acid; 9 = terbutaline; 10 = atenolol; 11 = arginine-vasopressin. The $\text{ether-IAM.PC}_{10/C_3}$ column was 15×0.46 cm and the mobile phase was 0.01 M PBS (pH 7.4).

Using eleven experimental drugs, IAM chromatography also predicted oral absorption in mice. Fig. 6A shows that for a set of eleven cephalosporin prodrugs (Table 3), $\log(k'_{IAM})$ correlates well with $\log(\% \text{ Oral Abs})$ with $r = 0.941$, whereas an ODS column gave a correlation of $r = 0.890$ (Fig. 6B). Although IAM chromatography is slightly better than ODS chromatography, the key finding is that the evaluation of drugs by IAM chromatography is much easier than ODS chromatography. This is because the capacity factor data in Fig. 4 all correspond to mobile-phase conditions that are completely aqueous. Some compounds required acetonitrile for elution, and the capacity factors from several isocratic elutions at different acetonitrile concentrations were necessary to obtain the theoretical capacity factors at pure aqueous condition. Linear extrapolation of plots of $\log(\text{capacity factor})$ vs. $\log(\% \text{ acetonitrile})$ gives the capacity factor at 0% acetonitrile [31]. This extrapolation

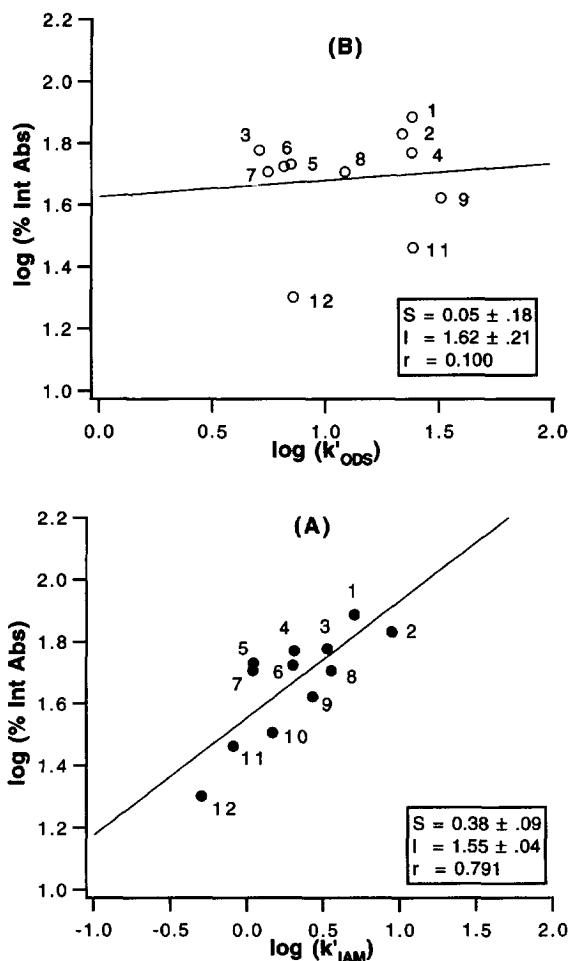


Fig. 5. Correlation of rat intestinal drug absorption [30] with drug partitioning to an $\text{ether-IAM.PC}_{10/C_3}$ column [$\log(k'_{IAM})$] or ODS columns [$\log(k'_{ODS})$]. $\log(\% \text{ Int Abs})$ correlates with $\log(k'_{IAM})$ with $r = 0.791$ (A), but does not correlate with $\log(k'_{ODS})$ $r = 0.1$ (B). The twelve drugs tested in this experiment are the following: 1 = *m*-nitroaniline; 2 = *p*-nitroaniline; 3 = salicylic acid; 4 = *p*-toluidine; 5 = aniline; 6 = *m*-nitrobenzoic acid; 7 = benzoic acid; 8 = phenol; 9 = acetanilide; 10 = antipyrine; 11 = theophylline; 12 = acetylsalicylic acid. The $\text{ether-IAM.PC}_{10/C_3}$ column was 15×0.46 cm and the mobile phase was 0.01 M PBS (pH 5.4).

method was needed for nine of the eleven drugs on the ODS column and only two of the eleven drugs on the IAM column. Thus the IAM column not only gives a better correlation than ODS columns (Fig. 5), but IAM chromatography usually does not require the data collection needed for extrapolation to 0% acetonitrile.

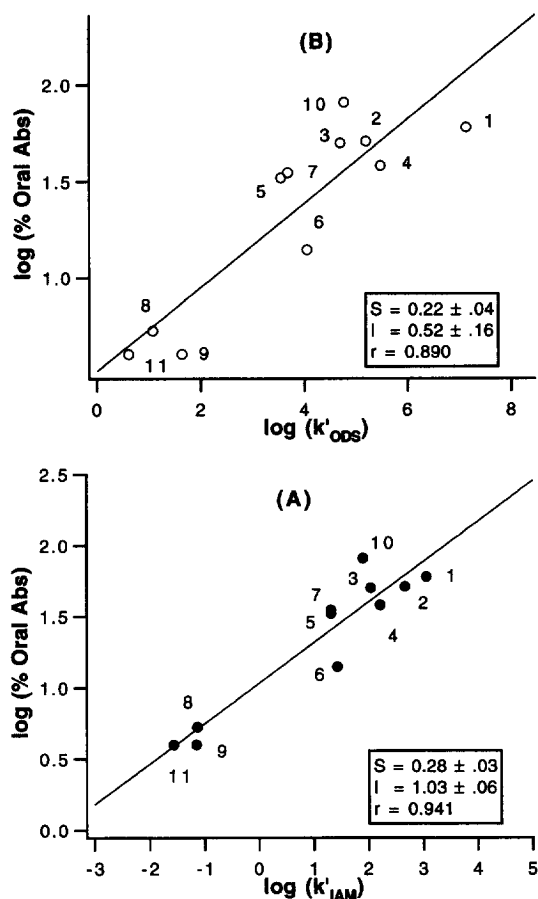
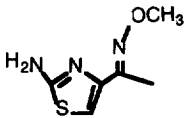
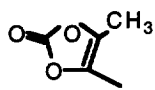
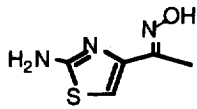
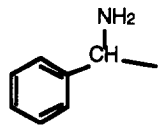


Fig. 6. Correlation of oral drug absorption in mice with drug partitioning to an ^{ether}IAM.PC_{10/C3} column [$\log(k'_{IAM})$] or ODS column [$\log(k'_{ODS})$]. k'_{IAM} and k'_{ODS} were measured on a 3 cm \times 0.46 cm ^{ether}IAM.PC_{10/C3} column and a 3 \times 0.46 cm ODS column, respectively, using a mobile phase of 0.01 M PBS buffered at pH 7.4 except for compounds 1 and 2, and compounds 1–8 and 10 for the ODS column, which did not elute with an aqueous phase. For the compounds not eluting with an aqueous mobile phase, four concentrations of acetonitrile were used as isocratic mobile phases and linear plots of $\log(k'_x)$ vs. x were extrapolated to the x coordinate to obtain k'_{IAM} or k'_{ODS} that theoretically corresponds to 0% acetonitrile. All data given represent k' values corresponding to 100% aqueous mobile phases. Oral absorption of these drugs was measured as described [33].

An important finding from this study is that IAM chromatography always gives better correlations than ODS chromatography or octanol–water partitioning systems regarding modeling the interactions of drugs with fluid membranes. In support of this, the intestinal transport of

Table 3
Structures of cephalosporin prodrugs

	R ₁	R ₂
1. LY211193	- CHOCOCH ₂ CH(CH ₃) ₂ CH(CH ₃) ₂	
2. LY257290	- CHOCOOCHCH ₃ CH ₃	CH ₂ CH ₂ CH ₃
3. LY249902	- CHOCOOCH(CH ₃) ₂ CH ₃	
4. LY248722	- CHOCOC(CH ₃) ₃ CH ₃	
5. LY267858	- CHOCOCH ₃ CH ₃	
6. LY223653		
7. LY264568	H	
8. LY231378	- CHOCOOCH(CH ₃) ₂ CH ₃	
9. LY191297	H	
10. LY264830	CH ₂ O ₂ CC(CH ₃) ₃	
11. LY227060	H	

eleven structurally unrelated drugs (Fig. 5) was predicted by IAM chromatography but not ODS chromatography. The oral absorption of eleven structurally similar drugs (Fig. 6B) gave acceptable correlations when modeled on either ODS or IAM columns, but IAM chromatography gave

a better correlation and in addition, the experimental data was much easier to obtain.

The main conclusion from this work is that drug partitioning into IAM surfaces correlates with oral drug absorption in mice and also drug permeability through Caco-2 cells; drug permeability through Caco-2 cells correlates with the clinical absorption of drugs [1]. Thus, IAMs may be useful for predicting drug absorption in humans.

3.3. Mechanism of solute retention on IAM chromatography

As discussed above, drug transport across membranes depends on the partitioning of the drug into the membrane. Solute–membrane partitioning represents one of the major membrane processes controlling the membrane transport of solute molecules. This is because membrane partitioning accounts for solute's penetration through the headgroup region of IAMs. In contrast to the partitioning process, adsorption of solutes on the membrane surface is also possible. Thus solute–IAM interactions may be dominated by either partitioning, adsorption, or both. It is clear that partitioning is the prerequisite of solute transport across the membrane because if solute–membrane interactions are dominated by only adsorption, the solute will not transport across the membrane. Elucidating the solute retention mechanism on IAMs is thus critical to understand why IAM surfaces can be used to predict drug transport across membranes.

Three IAM.PC bonded phases with different bonded ligand densities were used to study the mechanism of solute retention on IAM columns. The chemical structures of these three IAM.PC phases are shown in Scheme 1 and the bonded ligand densities of these three IAM.PC phases were shown in Table 1. Figs. 7A–C compare the retention k'_{IAM} values of sixteen solutes on three different IAM.PC columns. There is almost a perfect correlation ($r^2 > 0.99$) between k'_{IAM} values obtained on the $^{ether}IAM.PC^{C_{10}/C_3}$ column and k'_{IAM} values obtained on the IAM.PC.DD column (Fig. 7A). Similar results were found when correlating solute retention between

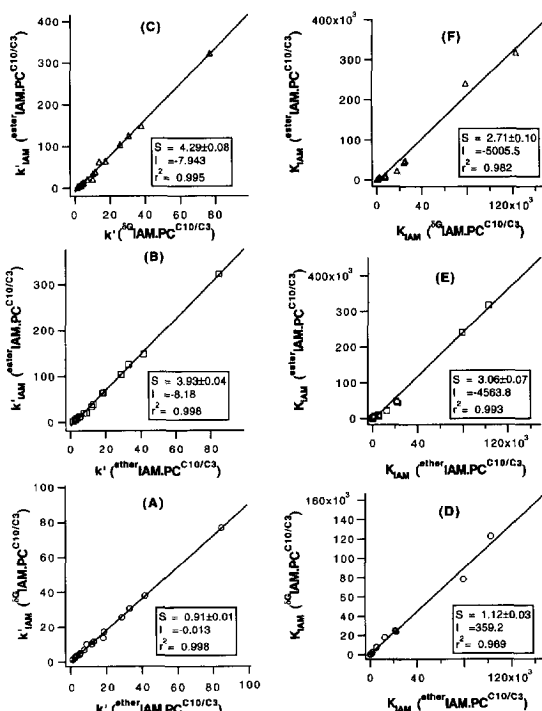


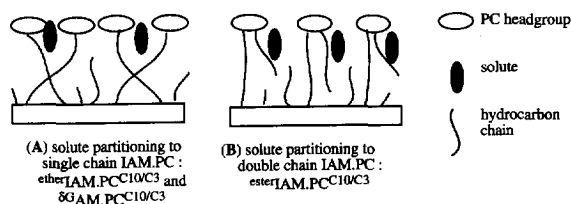
Fig. 7. Correlation of the IAM capacity factors (k'_{IAM}) of 16 solutes including five *p*-alkylphenols (phenol, *p*-cresol, *p*-ethylphenol, *p*-*n*-propylphenol, *p*-*n*-butylphenol), four *p*-halophenols (*p*-fluorophenol, *p*-chlorophenol, *p*-bromophenol, *p*-iodophenol), and seven β -blockers (atenolol, pindolol, nadolol, metoprolol, oxprenolol, alprenolol, propranolol) on the single chain and double chain IAM.PC columns at 298 K (A–C), and correlation of the equilibrium distribution constant of 16 solutes on the single chain and double chain IAM.PC columns at 298 K (D–F). All three IAM.PC columns were 3×0.46 cm and the mobile phase was 0.01 M PBS buffer (pH 7.4).

$^{ester}IAM.PC^{C_{10}/C_3}$ and $^{ether}IAM.PC^{C_{10}/C_3}$ columns (Fig. 7B) and $^{ester}IAM.PC^{C_{10}/C_3}$ and IAM.PC.DD columns (Fig. 7C). More important, the slope of 0.91 in Fig. 7A indicates that k'_{IAM} capacity factors measured on single chain IAM.PC.DD and $^{ether}IAM.PC^{C_{10}/C_3}$ columns are virtually identical. However, the slopes of ca. 4 in Fig. 7B and C indicate that the double chain $^{ester}IAM.PC^{C_{10}/C_3}$ column has a ca. 4-fold higher k'_{IAM} value compared to the single chain IAM columns.

The IAM capacity factors k'_{IAM} can be used to

calculate the K_{IAM} values which reflect the distribution of solute between the stationary phase and the mobile phase according to Eq. 4 and also using the phase ratio ($\phi = V_s/V_m$) values of 0.046 for $^{ether}IAM.PC^{C_{10}/C_3}$, 0.035 for IAM.PC.DD, and 0.053 for $^{ester}IAM.PC^{C_{10}/C_3}$ [24]. The K_{IAM} values obtained on each IAM column correlate with the K_{IAM} values obtained with the other two IAM columns (Fig. 7D–F); excellent linear correlations ($r^2 = 0.982$ – 0.998) were always obtained. It should be noted that the affinity of solutes for the $^{ester}IAM.PC^{C_{10}/C_3}$ surface is about three times the affinity of solutes for the $^{ether}IAM.PC^{C_{10}/C_3}$ surface or the IAM.PC.DD surface (Fig. 7E, F). These results are significant and provide insight into the mechanism of solute retention as further discussed below.

As shown in Scheme 4, the outermost surface of IAM.PC contains a monolayer of PC headgroups, and underneath these polar lipid headgroups reside the hydrocarbon chains from the immobilized PC, C_{10} , and C_3 ligands. If solute adsorption dominates retention, the amount of immobilized PC headgroups determines k'_{IAM} . The density of PC headgroups on the $^{ester}IAM.PC^{C_{10}/C_3}$ column (98 $\mu\text{mol-PC/g-IAM}$, Table 1) is lower than the densities of PC headgroups on $^{ether}IAM.PC^{C_{10}/C_3}$ or IAM.PC.DD (127 $\mu\text{mol-PC/g-IAM}$). Based on PC headgroup density an adsorption retention mechanism predicts that the $^{ester}IAM.PC^{C_{10}/C_3}$ column should have the lowest affinity for the solutes. However, Fig. 7E and F demonstrated the opposite effect, i.e., the $^{ester}IAM.PC^{C_{10}/C_3}$ column has the highest affinity for the solutes. The higher retention of solutes on the $^{ester}IAM.PC^{C_{10}/C_3}$ column compared to the other single chain IAM columns indicates that solute



Scheme 4.

partitioning, instead of solute adsorption, dominates the mechanism of retention on IAMs.

The above results indicate that for these solutes a partitioning mechanism controls solute retention on the IAM phase. Thus the solute actually penetrates beyond the interfacial PC headgroups and is embedded within the IAM.PC bonded phase (Scheme 3). The interfacial PC headgroups may function as a barrier to the solute partitioning process. Thus, the higher solute affinity on the ester column may be the result of a lower immobilized PC density that exhibits a lower interfacial barrier to solute penetrating into the IAM hydrocarbon region. This is also consistent with the results in Fig. 1 which show that the IAM partition coefficient (K_{IAM}) for solute partitioning into $^{ether}IAM.PC^{C_{10}/C_3}$ column is about seven times higher than the liposome partitioning coefficient (K_m) (Eq. 6). These results suggest that the density of the PC headgroup is one of the most important factors responsible for the solute partitioning into phospholipid membranes [24]. The PC membrane with a lower PC headgroup density exhibits a lower interfacial barrier to solute partitioning and thus favors solute partitioning. A comparison of solute partitioning into DMPC liposomes and the three IAM.PC phases is given below.

	$^{ester}IAM.PC^{C_{10}/C_3}$	$^{ether}IAM.PC^{C_{10}/C_3}$ or IAM.PC.DD	DMPC liposomes
Density of lipid headgroup (surface area/PC)	ca. 105 Å	ca. 85 Å	ca. 62 Å [29]
Membrane partition coefficient	ca. 20 K_m	ca. 7 K_m	K_m

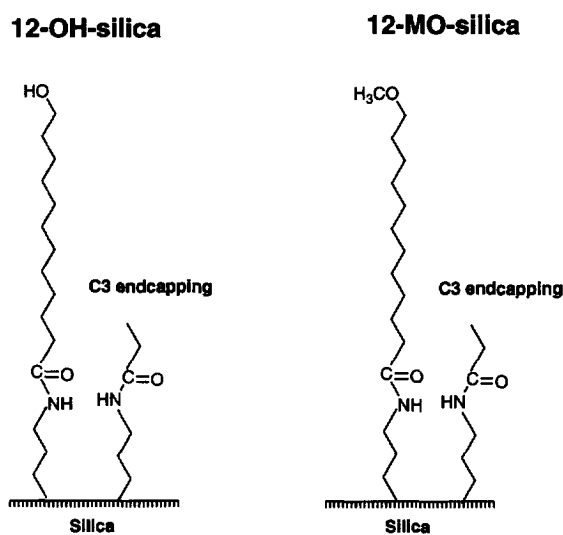
3.4. Structural requirements of chromatographic surfaces for modeling membrane partitioning

The results in Fig. 7 not only provide insight into the solute retention mechanism on IAMs as discussed above, but also provide very valuable information regarding the structural requirements of immobilized PC ligand needed to predict solute–membrane partitioning. The key question is: what are the lipid structural requirements for an HPLC surface to predict solute partitioning into biological membranes? As shown in Scheme 1, the immobilized PC ligand comprising the ^{ester}IAM.PC^{C₁₀/C₃} surface is a diacylated ester PC, whereas the immobilized PC ligands comprising ^{ether}IAM.PC^{C₁₀/C₃} and IAM.PC.DD are single chain PC analogs with and without the glycerol backbone, respectively. In spite of these structural differences, all three IAM.PC surfaces shown in Scheme 1 give virtually identical rank orders of the solute–membrane partitioning (Fig. 7), and thus give virtually identical results in predicting drug partitioning into fluid DMPC liposomes [22,24]. The key point is that although solute retention times are different for these three IAM.PC columns, the biological membrane partitioning process is predicted equally well on all three different IAM.PC columns. Thus the glycerol backbone, the linkage between the glycerol backbone and the acyl chain linkage (ether linkage or ester linkage), and the number of acyl chains are not critical structural features of surfaces to evaluate solute partitioning into membranes containing phosphocholine analogs (i.e., DMPC liposomes).

A natural question arising from the above finding is whether surfaces prepared by immobilized ligands with polar groups other than PC protruding from the surface can be a good membrane model. In particular, since octanol–water partitioning systems have previously been extensively used to predict drug–membrane interactions prior to IAM chromatography, we speculated that immobilized octanol may create a surface that is a good membrane model. To address this question, we synthesized 12-hydroxy dodecanoic silica propyl amide (denoted as 12-OH-silica) and evaluated the capability of this

surface to predict drug partitioning into *n*-octanol–water phases, and also to predict drug partitioning into fluid membranes [12]. 12-OH-silica is effectively immobilized alcohol and can be considered as a solid-phase model of the *n*-octanol–water partitioning system. 12-OH-silica contains both hydrogen bond donor and acceptor capabilities at the surface. To probe the effect of H-bonding at the chromatographic interface, a surface lacking hydrogen bond donor capabilities was also prepared by immobilizing 12-methoxy dodecanoic acid (12-MO) on silica propyl amine to form 12-MO-silica. The general structures of 12-OH-silica and 12-MO-silica are shown in Scheme 5, which shows that monolayers of OH groups form on the 12-OH-silica surface and monolayers of OCH₃ groups form on the 12-MO-silica surface.

Fig. 8 shows the correlations between drug partitioning into DMPC liposomes [15,17,26] with drug partitioning into 12-OH-silica, and 12-MO-silica using 22 solutes shown in Scheme 2. It is clear by comparing Fig. 1 and Fig. 8 that the ^{ether}IAM.PC^{C₁₀/C₃} column predicted drug partitioning into DMPC liposomes ($r = 0.907$, Fig. 1) better than 12-OH-silica ($r = 0.812$, Fig. 8A), and 12-MO-silica ($r = 0.817$, Fig. 8B). Similar results were found for comparing the capability of these bonded phases to predict intestinal transport in



Scheme 5.

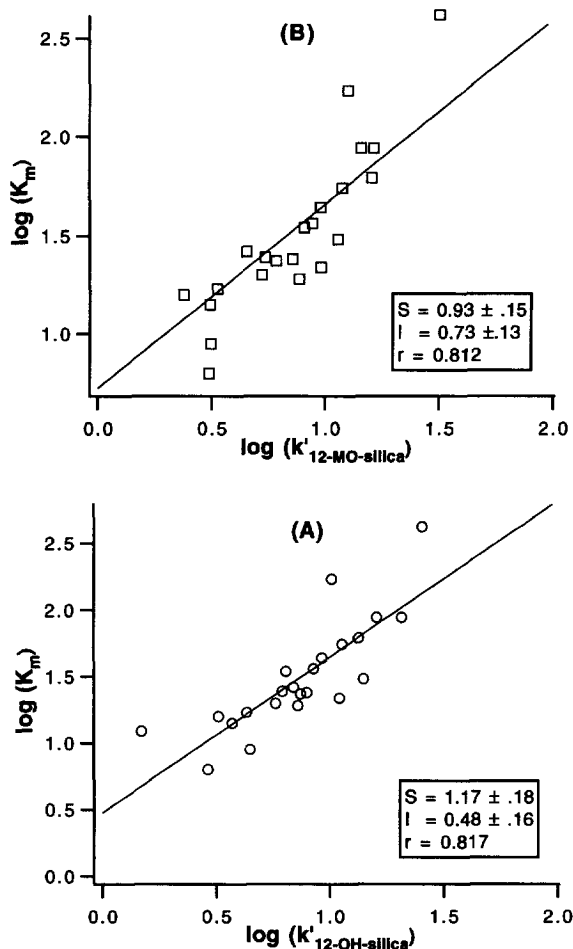


Fig. 8. Correlation of solute partitioning into DMPC liposomes [$\log(K_m)$] with solute partitioning into 12-OH-silica bonded phase [$\log(k'_{12\text{-OH-silica}})$] (A) and 12-MO-silica bonded phase [$\log(k'_{12\text{-MO-silica}})$] (B) 23 solutes shown in Scheme 2. The liposome partition coefficients of these 23 solutes were measured using DMPC liposomes dispersed in 0.01 M PBS buffer (pH 7.4) [15,17,26]. The capacity factors, $k'_{12\text{-OH-silica}}$, were measured on a 3×0.46 cm 12-OH-silica column, whereas the capacity factors, $k'_{12\text{-MO-silica}}$, were measured on a 15×0.46 cm 12-MO-silica column using a mobile phase of 0.01 M PBS (pH 7.4).

situ tissue models. For instance, the correlation between drug intestinal absorption and drug partitioning using $^{\text{ether}}\text{IAM.PC}^{C_{10}/C_3}$ ($r = 0.791$, Fig. 5A) was better than the correlation using the 12-OH-silica column ($r = 0.590$, Fig. 9A) and the 12-MO-silica column ($r = 0.681$, Fig. 9B). Most importantly, drug partitioning into non-polar

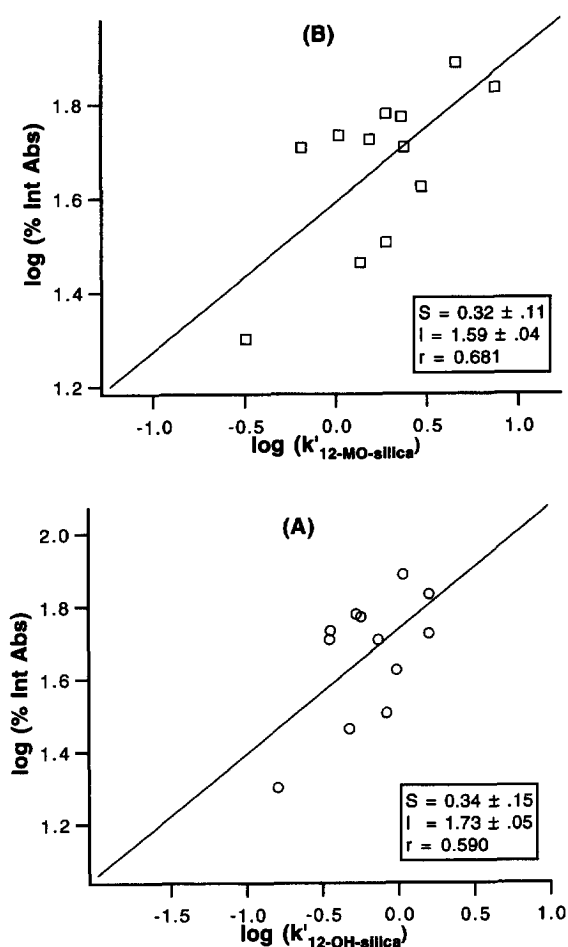


Fig. 9. Correlation of rat intestinal drug absorption [30] with solute partitioning into 12-OH-silica bonded phase [$\log(k'_{12\text{-OH-silica}})$] (A) and 12-MO-silica bonded phase [$\log(k'_{12\text{-MO-silica}})$] (B). The 12 drugs tested in this experiment are the following: *m*-nitroaniline, *p*-nitroaniline, salicylic acid, *p*-toluidine, aniline, *m*-nitrobenzoic acid, benzoic acid, phenol, acetanilide, antipyrine, theophylline, acetylsalicylic acid. The capacity factors, $k'_{12\text{-OH-silica}}$, were measured on a 3×0.46 cm 12-OH-silica column, whereas the capacity factors, $k'_{12\text{-MO-silica}}$, were measured on a 15×0.46 cm 12-MO-silica column using a mobile phase of 0.01 M PBS (pH 5.4).

ODS did not correlate with drug intestinal absorption ($r = 0.100$, Fig. 5B).

The above results indicate that $^{\text{ether}}\text{IAM.PC}^{C_{10}/C_3}$ better predicts drug-membrane interactions than 12-OH-silica and 12-MO-silica columns. This is because drug-IAM interactions involve not only hydrogen-bonding, Van

der Waal interactions, but also electrostatic interactions. Although 12-OH-silica and 12-MO-silica have hydrogen-bonding acceptors and donors, these surfaces can not model electrostatic interactions common between drug molecules and membranes that occur during the partitioning process. IAM.PC contains the zwitterionic PC headgroup and thus can model virtually all of the molecular interactions found in cell membranes during drug partitioning. It was thus expected that the IAM.PC phase would model the partitioning process because this phase contains the phosphocholine headgroup found in biological membranes. However, it was very surprising that 12-OH-silica and 12-MO-silica could model drug–membrane interactions significantly better than ODS reversed-phase columns.

It was even more surprising to find that there was almost no correlation between drug partitioning into 12-OH-silica and drug partitioning into *n*-octanol–water for the 22 solutes shown in Scheme 2 ($r = 0.297$, Fig. 10). 12-OH-silica is effectively immobilized alcohol and might be considered as a solid-phase model of the *n*-octanol–water partitioning system. The reason that 12-OH-silica does not model solute partitioning into octanol–water is that, although the chemical structure of the individual molecules in both 12-OH-silica and the octanol liquid phase are similar (i.e., both are fatty acid alcohols), the molecular assemblies in these two systems are completely different. In *n*-octanol–water systems, the octanol phase is a bulk liquid phase with octanol molecules randomly oriented with extensive configurational entropy of the system (Scheme 6A). In contrast, 12-OH-silica bonded phases are an ordered liquid having immobilized alcohol molecules arranged in a monolayer structure with OH groups protruding from the silica surface (Scheme 6B). Obviously, the physico-chemical properties of the immobilized alcohols on the 12-OH-silica surface are different compared to the non-bonded randomly oriented octanol molecules in the *n*-octanol–water system. Therefore, drug–12-OH-silica interactions are not expected to be similar to the drug–octanol interactions in the octanol–water system, as shown in Fig. 10.

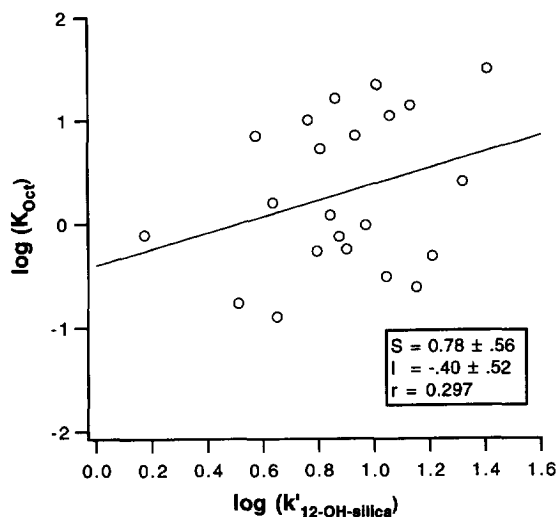
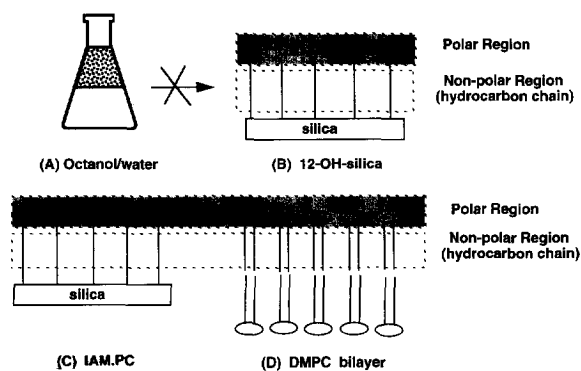


Fig. 10. Comparison of drug partitioning in 12-HO-silica [$\log(k'_{12\text{-HO-silica}})$] and drug partitioning in *n*-octanol–buffer phase for 22 drugs. 12-HO silica capacity factors, $k'_{12\text{-HO-silica}}$, were measured on a 3×0.46 cm 12-HO-silica column using a mobile phase of 0.01 M PBS (pH 7.4). The *n*-octanol–buffer partition coefficients of these drugs were measured elsewhere [15,17,26] using a 0.01 M PBS (pH 7.4) as buffer.

The differences in the molecular assemblies of 12-OH-silica and octanol phase in the octanol–water partitioning system also explain why drug partitioning into the immobilized alcohol phase correlates well with drug partitioning into DMPC liposomes (Fig. 8A), whereas drug partitioning into the octanol–water system does not correlate with drug partitioning into DMPC liposomes (Fig. 2A). This is because the ordered structure



Scheme 6.

of the membrane bilayer is important in drug–membrane interactions [14]. The 12-OH-silica surface is an ordered liquid containing a polar region and a non-polar region (Scheme 6B), which is similar to the interfacial molecular assemblies of the IAM.PC and DMPC bilayer. As shown in Schemes 6C and 6D, both IAM.PC and DMPC liposome are interfacial layered structures containing distinct polar and nonpolar regions.

In summary, an ordered monolayer of immobilized lipids containing both a polar and non-polar region is critical for a chromatographic surface to exhibit molecular recognition properties of biological membranes (Scheme 6). Surface PC headgroups, surface OH groups, and surface OCH₃ groups all provide the interfacial properties necessary to predict drug membrane interactions better than reversed-phase C₁₈ surfaces. However, when the interfacial polar region is comprised of the phospholipid headgroup found in biological membranes (i.e., not monolayers of -OH groups or OCH₃ groups), optimum membrane recognition properties are found for that surface. Thus IAM.PC was the best in vitro screen for predicting drug–membrane interactions compared to 12-OH-silica and 12-MO-silica bonded phases. In other words, the capability of these chromatographic surfaces to predict drug–membrane interactions parallels their ability to model the drug–membrane interactions at the surface as shown below.

4. Conclusion

Solute partitioning into fluid liposome membranes can be modeled by solute partitioning into IAMs, and the solute–membrane partitioning can be chromatographically measured using IAM surfaces. On the base of this finding, IAM chromatography has been demonstrated as a novel and simple in vitro screen for predicting drug membrane permeability. In addition, a recent report demonstrated that IAMs can predict pharmacokinetic parameters including drug binding to proteins [Kaliszan, 1994 No. 44], and therefore, IAM chromatography may be useful in QSAR studies.

Acknowledgements

We are very grateful for the support from Eli Lilly and Company. This work was also supported by NSF (CTS 9214794), NIH (AI33031), and Regis Technologies (2R446M3022-02). We are also very grateful for the gifts of the imidazolidine derivatives (ST drugs) from Boehringer-Ingelheim and the gifts phenethylamine derivatives from Dr. D. Nichols of the Department of Medicinal Chemistry at Purdue University.

Bonded phases	IAM.PC	12-MO-silica	12-OH-Silica	ODS
Types of molecular interactions modeled	Van der Waals hydrogen bonding electrostatic steric effects dipole–dipole	Van der Waals Hydrogen bonding dipole–dipole	Van der Waals Hydrogen bonding dipole–dipole	Van der Waals
Ability to predict drug–membrane interactions	Good	Moderate	Moderate	Poor

Abbreviations

12-MO-silica	12-methoxy dodecanoic silica propyl amide
12-OH-silica	12-hydroxy dodecanoic silica propyl amide
C_3	propionyl
C_{10}	decanoyl
D	diffusion coefficient
D_m	membrane diffusion coefficient
DMPC	dimyristoylphosphatidylcholine
HPLC	high-performance liquid chromatography
IAM(s)	immobilized artificial membrane(s)
k'	capacity factor or retention factor
k'_{IAM}	capacity factor on IAM column
k'_{ODS}	capacity factor on ODS column
K	partition coefficient
K_{IAM}	IAM partition coefficient
K_m	membrane (liposome) partition coefficient
K_{oct}	octanol–water partition coefficient
ODS	octadecyl silica
P_m	permeability coefficient
PBS	phosphate-buffered saline
QSAR	quantitative structure–activity relationship
S	slope in linear least-square fitting
SPA	silica propylamine

References

- [1] P. Artursson and J. Karlsson, *Biochem. Biophys. Res. Commun.*, 175 (1991) 880.
- [2] W.D. Stein, *Transport and Diffusion across Cell Membranes*, Academic Press, Orlando, FL, 1986.
- [3] C. Hansch and W.J. Dunn, *J. Pharm. Sci.*, 61 (1972) 1.
- [4] C. Hansch, R.M. Muri, T. Fujita, P.P. Maloney, F. Geiger and M. Streich, *J. Am. Chem. Soc.*, 85 (1963) 2817.
- [5] C. Hansch and J.M. Clayton, *J. Pharm. Sci.*, 62 (1973) 1.
- [6] T. Braumann, *J. Chromatogr.*, 373 (1986) 191.
- [7] W. Butte, C. Fookan, R. Klusmann and D. Schuller, *J. Chromatogr.*, 214 (1981) 59.
- [8] R. Gami-Yilinkou, A. Nasal and R. Kaliszan, *J. Chromatogr.*, 633 (1993) 57.
- [9] Y. Katz and J.M. Diamond, *J. Membrane Biol.*, 17 (1974) 101.
- [10] Y. Katz and J.M. Diamond, *J. Membrane Biol.*, 17 (1974) 87.
- [11] Y. Katz and J.M. Diamond, *J. Membrane Biol.*, 17 (1974) 67.
- [12] H. Liu, S. Ong, L. Glanz and C. Pidgeon, *Anal. Chem.* (1995) submitted.
- [13] W.J. Pjura, A.M. Kleinfeld and M.J. Karnovsky, *Biochemistry*, 23 (1984) 2039.
- [14] L. De Young and K.A. Dill, *Biochemistry*, 27 (1988) 5281.
- [15] Y.W. Choi and J.A. Rogers, *Pharm. Res.*, 7 (1990) 508.
- [16] G.V. Betageri and J.A. Rogers, *Pharm. Res.*, 6 (1989) 399.
- [17] G.V. Betageri and J.A. Rogers, *Pharm. Res.*, 10 (1993) 913.
- [18] S. Ong, S.J. Cai, C. Bernal, D. Rhee, X. Qiu and C. Pidgeon, *Anal. Chem.*, 66 (1994) 782.
- [19] D. Rhee, M.R., W.G. Chae, X. Qiu and C. Pidgeon, *Anal. Chim. Acta*, 297 (1994) 377.
- [20] X. Qiu and C. Pidgeon, *J. Phys. Chem.*, 97 (1993) 12399.
- [21] S. Ong, X. Qiu and C. Pidgeon, *J. Phys. Chem.*, 98 (1994) 10189.
- [22] S. Ong, H. Liu, X. Qiu, G. Bhat and C. Pidgeon, *Anal. Chem.*, 67 (1995) 755.
- [23] C. Pidgeon, S. Ong, H. Liu, X. Qiu, M. Pidgeon, A.H. Dantzig, J. Munroe, W.J. Hornback, J.S. Kasher, L. Glunz and T. Szczerba, *J. Med. Chem.*, 38 (1995) 590.
- [24] S. Ong and C. Pidgeon, *Anal. Chem.* (1995) in press.
- [25] C. Pidgeon and U.V. Venkatarum, *Anal. Biochem.*, 176 (1989) 36.
- [26] G.V. Betageri and J.A. Rogers, *Int. J. Pharm.*, 36 (1987) 165.
- [27] L.A. Cole and J.G. Dorsey, *Anal. Chem.*, 64 (1992) 1317.
- [28] W. Cheng, *Anal. Chem.*, 57 (1985) 2409.
- [29] R.P. Rand and V.A. Parsegian, *Biochim. Biophys. Acta*, 998 (1989) 351.
- [30] L.S. Schanker, D.J. Tocco, B.B. Brodie and C.A.M. Hogben, *J. Pharmacol. Exp. Ther.*, 123 (1958) 81.
- [31] D. Schmidt, J.H. Votaw, R.M. Kessler and T. De Paulis, *J. Pharm. Sci.*, 83 (1994) 305.
- [32] D.E. Nichols, A.T. Shulgin and D.C. Dyer, *Life Sci.*, 21 (1977) 569.
- [33] J.A. Eudaly, W.J. Hornback, R.J. Johnson, C.L. Jordan, J.E. Munroe, W.E. Wright and C.Y.E. Wu, in P.H. Bentley and R. Southgate (Editors), *Recent Advances in the Chemistry of Beta-Lactam Antibiotics*, The Chemical Society, London, 1989, p. 333.